



Measurement of the mass and lifetime of the Ω_b^- baryon

The LHCb collaboration[†]

Abstract

A proton-proton collision data sample, corresponding to an integrated luminosity of 3 fb^{-1} collected by LHCb at $\sqrt{s} = 7$ and 8 TeV, is used to reconstruct 63 ± 9 $\Omega_b^- \rightarrow \Omega_c^0 \pi^-$, $\Omega_c^0 \rightarrow p K^- K^- \pi^+$ decays. Using the $\Xi_b^- \rightarrow \Xi_c^0 \pi^-$, $\Xi_c^0 \rightarrow p K^- K^- \pi^+$ decay mode for calibration, the lifetime ratio and absolute lifetime of the Ω_b^- baryon are measured to be

$$\frac{\tau_{\Omega_b^-}}{\tau_{\Xi_b^-}} = 1.11 \pm 0.16 \pm 0.03,$$

$$\tau_{\Omega_b^-} = 1.78 \pm 0.26 \pm 0.05 \pm 0.06 \text{ ps},$$

where the uncertainties are statistical, systematic and from the calibration mode (for $\tau_{\Omega_b^-}$ only). A measurement is also made of the mass difference, $m_{\Omega_b^-} - m_{\Xi_b^-}$, and the corresponding Ω_b^- mass, which yields

$$m_{\Omega_b^-} - m_{\Xi_b^-} = 247.4 \pm 3.2 \pm 0.5 \text{ MeV}/c^2,$$

$$m_{\Omega_b^-} = 6045.1 \pm 3.2 \pm 0.5 \pm 0.6 \text{ MeV}/c^2.$$

These results are consistent with previous measurements.

Published in Phys. Rev. D93, 092007 (2016)

© CERN on behalf of the LHCb collaboration, licence CC-BY-4.0.

[†]Authors are listed at the end of this paper.

1 Introduction

Measurements of the lifetimes of beauty baryons provide an important test of Heavy Quark Effective Theory (HQET) [1–8], in which it is predicted that the decay width is dominated by the weak decay of the heavy b quark. The large samples of b baryons collected by LHCb have led to greatly improved measurements of their lifetimes [9–12], which are in good agreement with HQET predictions. In particular, the lifetime of the Λ_b^0 baryon is now measured to a precision of better than 1% [13], and those of the Ξ_b^0 and Ξ_b^- to about 3% [12, 13]. Within HQET it is expected that the lifetimes of weakly-decaying b baryons follow the hierarchy $\tau_{\Omega_b^-} \simeq \tau_{\Xi_b^-} > \tau_{\Xi_b^0} \approx \tau_{\Lambda_b^0}$ [14–16], and thus far, the measured lifetimes respect this pattern within the uncertainties. However, the uncertainty on the measured lifetime of the Ω_b^- baryon is too large to fully verify this prediction. The single best measurement to date of the Ω_b^- lifetime is $1.54_{-0.21}^{+0.26} \pm 0.05$ ps [10] by the LHCb experiment, based on a sample of 58 ± 8 reconstructed $\Omega_b^- \rightarrow J/\psi \Omega^-$ decays, with $J/\psi \rightarrow \mu^+ \mu^-$, $\Omega^- \rightarrow \Lambda K^-$ and $\Lambda \rightarrow p \pi^-$. Larger samples are needed to reduce the statistical uncertainty.

Improved knowledge of the Ω_b^- mass would provide tighter experimental constraints for tests of lattice quantum chromodynamics (QCD) and QCD-inspired models, which aim to accurately predict the masses of hadrons [17]. The two most recent measurements of the Ω_b^- mass, by the LHCb [18] and CDF [19] collaborations are in agreement, but an earlier measurement by the D0 collaboration [20] is larger by about 10 standard deviations.

In this paper, we report measurements of the mass and lifetime of the Ω_b^- baryon using the decay mode $\Omega_b^- \rightarrow \Omega_c^0 \pi^-$, where $\Omega_c^0 \rightarrow p K^- K^- \pi^+$. (Charge-conjugate processes are implied throughout.) The only prior evidence of the $\Omega_b^- \rightarrow \Omega_c^0 \pi^-$ decay has been in the $\Omega_c^0 \rightarrow \Omega^- \pi^+$ mode, with a signal of 4 events (3.3σ significance) [19]. The $\Omega_c^0 \rightarrow p K^- K^- \pi^+$ decay mode is Cabibbo suppressed and is yet to be observed. However, it has the advantage of a larger acceptance in the LHCb detector compared to decay modes with hyperons in the final state. For example, the yield of Ξ_b^- decays reconstructed using $\Xi_b^- \rightarrow \Xi_c^0 \pi^-$, $\Xi_c^0 \rightarrow p K^- K^- \pi^+$ decays [12] is about six times larger than that obtained using $\Xi_b^- \rightarrow J/\psi \Xi^-$ decays [10], where $\Xi^- \rightarrow \Lambda \pi^-$ and $\Lambda \rightarrow p \pi^-$.

The mass and lifetime measurements are calibrated with respect to those of the Ξ_b^- baryon, reconstructed in the $\Xi_b^- \rightarrow \Xi_c^0 \pi^-$, $\Xi_c^0 \rightarrow p K^- K^- \pi^+$ decay mode. The mass and lifetime of the Ξ_b^- are measured to be $m_{\Xi_b^-} = 5797.72 \pm 0.55$ MeV/ c^2 and $\tau_{\Xi_b^-} = 1.599 \pm 0.041 \pm 0.022$ ps [12], respectively; the measurements are of sufficiently high precision that they do not represent a limiting uncertainty in the Ω_b^- measurements presented here. The two quantities that are measured are the mass difference, $\delta m = m_{\Omega_b^-} - m_{\Xi_b^-}$, and the lifetime ratio $\tau_{\Omega_b^-}/\tau_{\Xi_b^-}$. The identical final states and similar energy release in the b and c baryon decays lead to a high degree of cancellation of the systematic uncertainties on these quantities. Throughout this article, we use X_b (X_c) to refer to either a Ξ_b^- (Ξ_c^0) or Ω_b^- (Ω_c^0) baryon.

2 Detector and simulation

The measurements use proton-proton (pp) collision data samples, collected by the LHCb experiment, corresponding to an integrated luminosity of 3.0 fb^{-1} , of which 1.0 fb^{-1} was recorded at a center-of-mass energy of 7 TeV and 2.0 fb^{-1} at 8 TeV. The LHCb detector [21, 22] is a single-arm forward spectrometer covering the pseudorapidity range $2 < \eta < 5$, designed for the study of particles containing b or c quarks. The detector includes a high-precision tracking system consisting of a silicon-strip vertex detector surrounding the pp interaction region, a large-area silicon-strip detector located upstream of a dipole magnet with a bending power of about 4 Tm, and three stations of silicon-strip detectors and straw drift tubes placed downstream of the magnet. The tracking system provides a measurement of momentum of charged particles with a relative uncertainty that varies from 0.5% at low momentum to 1.0% at 200 GeV/ c . The minimum distance of a track to a primary vertex (PV), the impact parameter (IP), is measured with a resolution of $(15 + 29/p_T) \mu\text{m}$, where p_T is the component of the momentum transverse to the beam, in GeV/ c . Different types of charged hadrons are distinguished using information from two ring-imaging Cherenkov detectors. Photons, electrons and hadrons are identified by a calorimeter system consisting of scintillating-pad and preshower detectors, an electromagnetic calorimeter and a hadronic calorimeter. Muons are identified by a system composed of alternating layers of iron and multiwire proportional chambers.

The online event selection is performed by a trigger [23], which consists of a hardware stage, based on information from the calorimeter and muon systems, followed by a software stage, which applies a full event reconstruction. The software trigger requires a two-, three- or four-track secondary vertex with a large p_T sum of the tracks and a significant displacement from the primary pp interaction vertices. At least one particle should have $p_T > 1.7 \text{ GeV}/c$ and be inconsistent with coming from any of the PVs. The signal candidates are required to pass a multivariate software trigger selection algorithm [24].

Proton-proton collisions are simulated using PYTHIA [25] with a specific LHCb configuration [26]. Decays of hadronic particles are described by EVTGEN [27], in which final-state radiation is generated using PHOTOS [28]. The interaction of the generated particles with the detector, and its response, are implemented using the GEANT4 toolkit [29] as described in Ref. [30]. The $\Xi_c^0 \rightarrow pK^-K^-\pi^+$ and $\Omega_c^0 \rightarrow pK^-K^-\pi^+$ decays are modeled as an equal mixture of $X_c \rightarrow pK^-\bar{K}^{*0}$, $\bar{K}^{*0} \rightarrow K^-\pi^+$ and $X_c \rightarrow pK^-K^-\pi^+$ (nonresonant) decays; this composition reproduces well the only clear structure in these decays, a \bar{K}^{*0} peak in the $K^-\pi^+$ mass distribution.

3 Candidate selection

Candidate $X_c \rightarrow pK^-K^-\pi^+$ decays are formed by combining four tracks consistent with this decay chain, and requiring a good quality vertex fit. In forming the X_c candidate, each particle must be significantly detached from all PVs in the event, have p_T greater than 100 MeV/ c , and have particle identification (PID) information consistent with the decay hypothesis. The PID requirements on the proton and the kaon candidates have a

combined efficiency of 70% on signal, while reducing the combinatorial background by a factor of 3.5.

Candidate X_b baryons are formed by combining an X_c candidate with a π^- candidate. For each X_b and PV pair in an event, a quantity $\chi_{\text{IP}}^2(X_b)$ is computed, defined as the increase in χ^2 when the X_b candidate is included as an additional particle in the PV fit. The X_b candidate is assigned to the PV with the smallest value of $\chi_{\text{IP}}^2(X_b)$, and it is required to be significantly displaced from that PV. The invariant mass $M(pK^-K^-\pi^+)$ is required to lie in the range 2461–2481 MeV/ c^2 and 2685–2705 MeV/ c^2 for Ξ_c^0 and Ω_c^0 signal candidates, respectively; these intervals cover a mass region that represents about ± 2.5 and ± 2.0 times the expected mass resolution. The tighter requirement on the Ω_c^0 candidates is used because of a lower signal-to-background ratio. Candidates for which the $pK^-K^-\pi^+$ mass is outside the signal region are also used to model the X_c combinatorial background contribution to the signal sample. To suppress combinatorial background, candidate X_b decays are required to have a reconstructed decay time larger than 0.2 ps, which is about five times the decay time resolution for these decays.

To further improve the signal-to-background ratio, a multivariate analysis is employed, based on a boosted decision tree (BDT) algorithm [31, 32] implemented within the TMVA package [33]. Simulated Ξ_b^- and Ω_b^- decays are used to represent the signal distributions, and background events are taken from the signal sidebands in data. The sidebands consist of events that are close in mass to the X_b signal region, but have either the $pK^-K^-\pi^+$ or $X_c\pi^-$ mass inconsistent with the known X_c or X_b masses. Independent training and test samples are used to ensure that the BDT is not overtrained.

A total of 18 discriminating variables are used to help differentiate signal and background candidates, including: the X_b decay vertex fit χ^2 ; the χ_{IP}^2 of the X_b , X_c and final-state decay products; the consistency of the candidate with being produced at one of the PVs in the event; the p_T of the decay products; and the PID information on the proton and two kaons. Due to differences in the PID information between simulation and data, the distributions of PID variables for signal are taken from $D^{*+} \rightarrow D^0\pi^+$ with $D^0 \rightarrow K^-\pi^+$, $\Lambda \rightarrow p\pi^-$ and $\Lambda_c^+ \rightarrow pK^-\pi^+$ decays in data [34], and are reweighted to account for differences in kinematics between the control and signal samples. The output of the training is a single discriminating variable that ranges from -1 to 1 . For convenience, the output value is also referred to as BDT.

The BDT requirement is chosen to maximize the figure of merit $N_S/\sqrt{N_S + N_B}$ for the Ω_b^- signal. Here, N_S and N_B are the expected signal and background yields as a function of the BDT requirement. The chosen requirement of $\text{BDT} > 0.3$ provides an expected signal (background) efficiency of about 90% (10%).

4 Mass spectra and fits

The X_c invariant mass spectra for X_b signal candidates are shown in Fig. 1. All candidates within the regions contributing to the Ω_b^- mass fit, 5420–6380 MeV/ c^2 , and the Ξ_b^- mass fit, 5630–6590 MeV/ c^2 , are included. The simulated distributions, normalized to the fitted

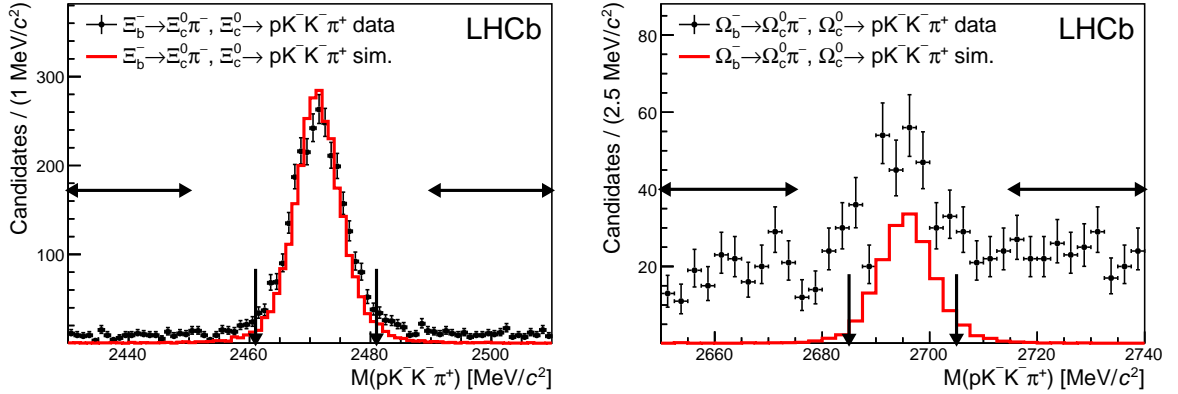


Figure 1: Invariant mass distribution for (left) $\Xi_c^0 \rightarrow pK^-K^-\pi^+$ and (right) $\Omega_c^0 \rightarrow pK^-K^-\pi^+$ candidates over the full X_b fit regions. The corresponding simulations (sim.) are overlaid. The vertical arrows indicate the signal regions, and the horizontal ones show the sideband regions.

number of X_c signal decays in data, are overlaid. The vertical and horizontal arrows indicate the signal and sideband regions.

While the overall background yields in these spectra are comparable, the signal-to-background ratio is much lower within the Ω_c^0 candidate sample due to the lower production rate of Ω_b^- relative to Ξ_b^- baryons, and likely a smaller $X_c \rightarrow pK^-K^-\pi^+$ branching fraction. Due to the very different X_c background levels for the signal and calibration mode, we use the X_c sidebands to model the X_c combinatorial background in the X_b invariant mass spectra.

To measure the Ω_b^- mass and yield, the data are fitted using a simultaneous extended unbinned maximum likelihood fit to four X_b invariant mass distributions; one pair is formed from the X_c signal regions, and the second pair comprises events taken from the X_c sidebands, as indicated in Fig. 1.

The signal shapes, determined from $\Omega_b^- \rightarrow \Omega_c^0\pi^-$ and $\Xi_b^- \rightarrow \Xi_c^0\pi^-$ simulated events, are each modeled by the sum of two Crystal Ball (CB) functions [35] which have a common mean value. The general forms of the two signal shapes are

$$\mathcal{F}_{\text{sig}}^{\Xi_b^-} = f_{\text{low}}\text{CB}_-(m_0, f_\sigma r_\sigma \sigma, \alpha_-, N_-) + (1 - f_{\text{low}})\text{CB}_+(m_0, f_\sigma \sigma, \alpha_+, N_+), \quad (1)$$

$$\mathcal{F}_{\text{sig}}^{\Omega_b^-} = f_{\text{low}}\text{CB}_-(m_0 + \delta m, r_\sigma \sigma, \alpha_-, N_-) + (1 - f_{\text{low}})\text{CB}_+(m_0 + \delta m, \sigma, \alpha_+, N_+). \quad (2)$$

Several of the parameters are common in the two signal shapes, and are determined from a simultaneous fit to the mass spectra from simulated samples of Ω_b^- and Ξ_b^- decays. The CB_\pm function represents the signal contribution with a tail toward low (-) or high (+) invariant mass. The parameters m_0 and $m_0 + \delta m$ represent the fitted peak mass values of the Ξ_b^- and Ω_b^- baryons, respectively; r_σ relates the lower CB width to the upper one; and f_σ allows for a small difference in the mass resolution for the signal and calibration modes. The exponential tail parameters α_\pm are common to the signal and calibration

modes. We fix the power-law tail parameters $N_- = N_+ = 10$, and the fraction $f_{\text{low}} = 0.5$, as the simulated signal shapes are well described without these parameters freely varied. In fits to the data, m_0 , δm and σ are left free to vary, and all other shape parameters are fixed to the values from the simulation.

Several sources of background contribute to the invariant mass spectrum for both the signal and the calibration modes. These include: (i) partially-reconstructed $X_b \rightarrow X_c \rho^-$ decays; (ii) misidentified $X_b \rightarrow X_c K^-$ decays; (iii) partially-reconstructed $\Omega_b^- \rightarrow \Omega_c^{*0} \pi^-$ decays (Ω_b^- only); (iv) random $X_c \rightarrow p K^- K^- \pi^+$ combinations; and (v) $X_b \rightarrow X_c \pi^-$ combinatorial background. The $X_b \rightarrow X_c \rho^-$ background shape is based on simulated decays, and is parameterized by an ARGUS distribution [36] convolved with a Gaussian resolution function of $16.4 \text{ MeV}/c^2$ fixed width, the value obtained from fully reconstructed $\Omega_b^- \rightarrow \Omega_c^0 \pi^-$ decays in data. The ARGUS shape parameters are left free to vary in the fit, as is the yield, expressed as a fraction of the $X_b \rightarrow X_c \pi^-$ yield. The $X_b \rightarrow X_c K^-$ background shape is fixed based on simulation. The yield fraction $N(X_b \rightarrow X_c K^-)/N(X_b \rightarrow X_c \pi^-)$ is fixed to 3.1%, which is the product of an assumed ratio of branching fractions $\mathcal{B}(X_b \rightarrow X_c K^-)/\mathcal{B}(X_b \rightarrow X_c \pi^-) = 7\%$, based on the value from Λ_b^0 decays [37], and the efficiency of the PID requirements on the K^- and π^- . The shape parameters used to describe these two backgrounds are common to the signal and calibration modes, apart from an overall mass offset, which is fixed to be equal to δm . The invariant mass distribution of the $\Omega_b^- \rightarrow \Omega_c^{*0} \pi^-$ background is taken from a parametrization of the mass distribution obtained from a phase-space simulation [38], combined with a Gaussian smearing based on the measured mass resolution. The yield fraction $N(\Omega_b^- \rightarrow \Omega_c^0 \pi^-)/N(\Omega_b^- \rightarrow \Omega_c^{*0} \pi^-)$ is freely varied in the fit to data.

The $X_c \rightarrow p K^- K^- \pi^+$ combinatorial background contribution is constrained by including the X_c sidebands in the simultaneous fit, as discussed above. The shape of this background is modeled by the sum of a broad Gaussian function and an exponential shape. In the X_c sidebands there is no indication of any Ξ_b^- or Ω_b^- contributions, which might result from nonresonant $X_b \rightarrow p K^- K^- \pi^+ \pi^-$ decays. The shape parameters and yields of this background component are freely varied in the fit, but their values are common for the X_c signal and sideband data samples. A different set of parameters is used for the Ω_b^- and Ξ_b^- decay modes. Random $X_c \pi^-$ combinatorial background is described by a single exponential function with variable slope and yield.

The X_b invariant mass spectra with the fits overlaid are shown in Fig. 2 for the X_c signal regions. The fitted yields are 62.6 ± 9.0 and 1384 ± 39 for the $\Omega_b^- \rightarrow \Omega_c^0 \pi^-$ and $\Xi_b^- \rightarrow \Xi_c^0 \pi^-$ modes, respectively. The $\Omega_b^- \rightarrow \Omega_c^0 \pi^-$, $\Omega_c^0 \rightarrow p K^- K^- \pi^+$ decay is observed for the first time with large significance, about 10 standard deviations based on Wilks's theorem [39]. The yield of $\Omega_b^- \rightarrow \Omega_c^0 \pi^-$ decays is comparable to that obtained in $\Omega_b^- \rightarrow J/\psi \Omega^-$ decays [10]. The mass difference is measured to be $\delta m = 247.7 \pm 3.0 \text{ MeV}/c^2$, where the uncertainty is statistical only.

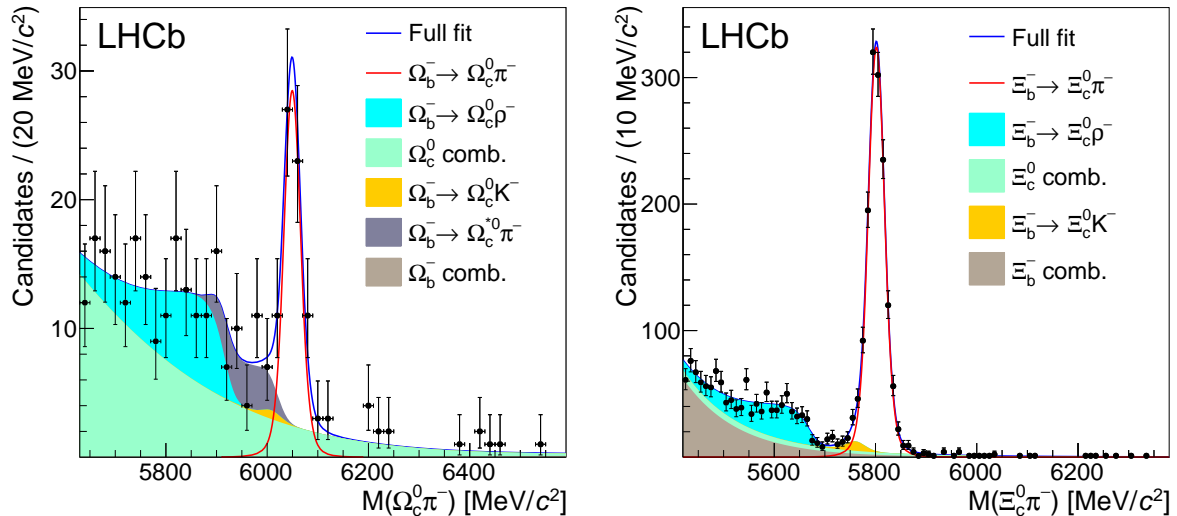


Figure 2: Results of the simultaneous mass fit to the signal and calibration modes. The fitted Ω_b^- combinatorial (comb.) background yield is very small, and not clearly visible.

Table 1: Results of the fit to data for each decay time bin, and the relative efficiency. The uncertainties are statistical only.

Decay time bin (ps)	Ω_b^- yield	Ξ_b^- yield	$\epsilon(\Xi_b^-)/\epsilon(\Omega_b^-)$
0.0–1.5	20.8 ± 4.8	450 ± 21	1.10 ± 0.03
1.5–2.5	12.0 ± 3.7	427 ± 21	1.11 ± 0.04
2.5–4.0	17.7 ± 4.2	305 ± 17	1.02 ± 0.04
4.0–12.0	10.5 ± 3.3	201 ± 14	1.03 ± 0.05

5 Ω_b^- lifetime

To measure the Ω_b^- lifetime, the data from the signal and calibration modes are divided into four bins of X_b decay time: 0.0–1.5 ps, 1.5–2.5 ps, 2.5–4.0 ps, and 4.0–12.0 ps. The decay time binning was chosen based on pseudoexperiments which replicate the yields of events in data as a function of decay time for the signal and calibration modes. Several binning schemes were investigated and the one above minimizes the systematic uncertainty on the lifetime due to the small Ω_b^- sample size.

The yields in each decay time bin in data are determined by repeating the mass fit for each decay time bin, allowing the signal and background yields to vary freely. All shape parameters are fixed to the values obtained from the fit to the whole data sample, since simulations show that they do not depend on the decay time. The results of the fits to the individual decay time bins are shown in Figs. 3 and 4 for the signal and calibration modes. The yields are presented in Table 1.

The relative efficiency in each bin is determined using simulated events. The efficiency-corrected yield ratio is then

$$\frac{N_{\Omega_b^- \rightarrow \Omega_c^0 \pi^-}(t)}{N_{\Xi_b^- \rightarrow \Xi^0 \pi^-}(t)} = A \exp(\kappa t), \quad (3)$$

where A is a calibration factor, and

$$\kappa \equiv 1/\tau_{\Xi_b^-} - 1/\tau_{\Omega_b^-}. \quad (4)$$

The value of κ is obtained by fitting an exponential function to the efficiency-corrected ratio of yields, which in turn allows $\tau_{\Omega_b^-}$ to be determined. The efficiencies for the signal and normalization modes are expressed as the fraction of generated signal decays with true decay time in bin i , which have a reconstructed decay time also in bin i . When defined in this way, effects of time resolution and selection requirements are accounted for, and the corrected signal and calibration mode yields are exponential in nature. The relative efficiencies after all selection requirements are given in Table 1.

The efficiency ratio is consistent with having no dependence on the decay time, as expected from the similarity of the two decay modes. The efficiency-corrected yield ratio as a function of decay time is shown in Fig. 5, along with a χ^2 fit to the data using an exponential function. The position of the points along the decay time axis is determined by taking the average value within the bin, assuming an exponential decay time distribution with $\tau = 1.60$ ps. From the fitted value of $\kappa = 0.053 \pm 0.085$ ps⁻¹ and the measured value of the Ξ_b^- lifetime, the lifetime ratio is found to be

$$\frac{\tau_{\Omega_b^-}}{\tau_{\Xi_b^-}} = \frac{1}{1 - \kappa \tau_{\Xi_b^-}} = 1.09 \pm 0.16, \quad (5)$$

where the uncertainty is statistical only.

6 Systematic uncertainties

A number of systematic uncertainties are evaluated, and are summarized in Table 2. Most of the systematic uncertainties are estimated by modifying each fixed input or function, and taking the difference with respect to the nominal value as the systematic uncertainty. The signal shape uncertainty is determined by changing the description to the sum of two Gaussian functions and repeating the analysis. The nominal X_c combinatorial background shape is changed from the sum of a Gaussian shape and an exponential function to a single exponential distribution. The sensitivity to the $\Omega_b^- \rightarrow \Omega_c^{*0} \pi^-$ shape description is investigated by varying the shape parameters obtained from the simulation to account for the uncertainty on the mass resolution, as well as using a different function to parametrize the simulation. The uncertainty on the yield of misidentified $X_b \rightarrow X_c K^-$ decays is quantified by varying the fractional contribution by $\pm 30\%$ relative to the nominal value, to allow for uncertainty in the $X_b \rightarrow X_c K^-$ branching fractions amongst these modes and

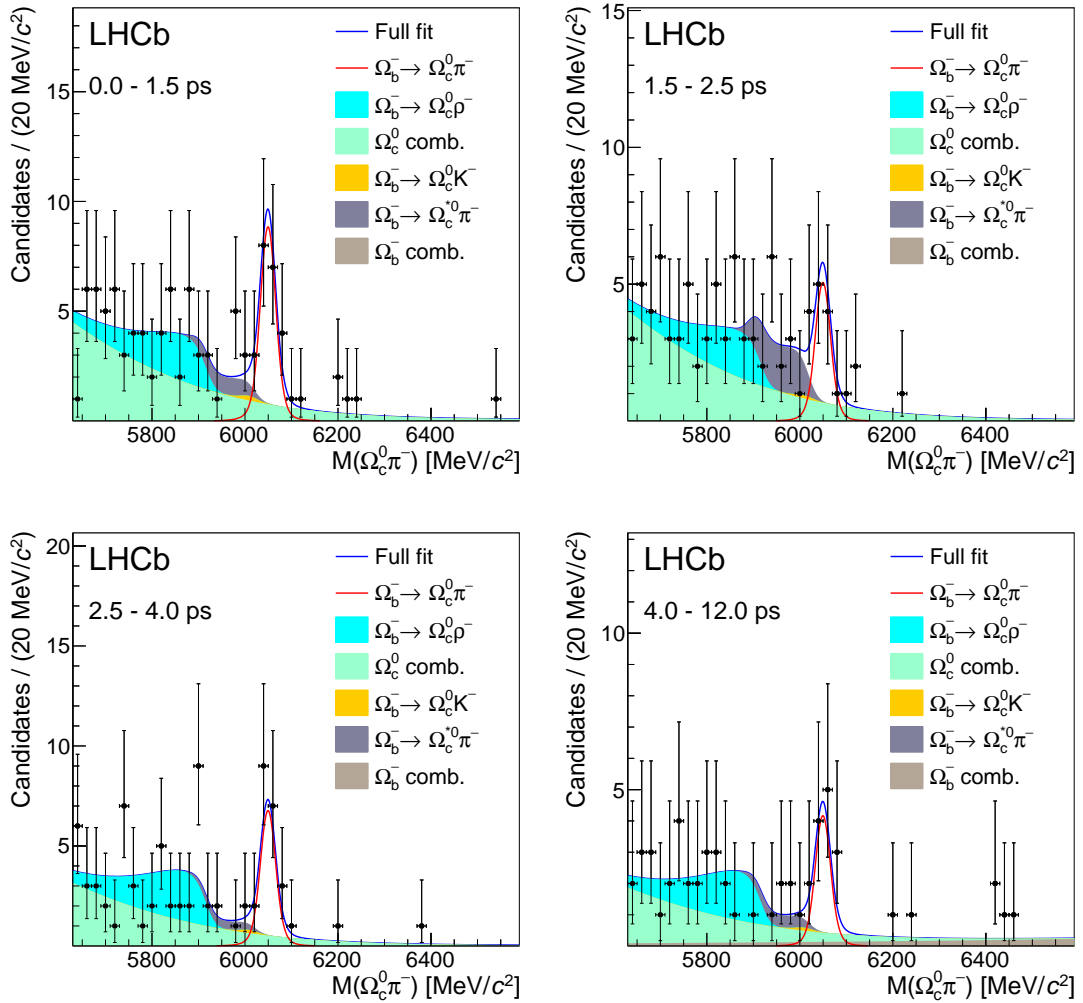


Figure 3: Results of the simultaneous mass fit to the Ω_b^- signal in the four decay time bins, as indicated in each plot.

for uncertainty in the PID efficiencies. The relative efficiency is obtained from simulation. However, the BDT performance in data is slightly worse than in simulation, so to estimate a potential bias in the lifetime ratio, we re-evaluate the relative efficiency with a $\text{BDT} > 0.6$ requirement, while keeping the nominal requirement on the data. This larger value was chosen since it provides equal efficiency of the BDT requirement on Ξ_b^- simulation as in data. To test the sensitivity to the position of the points along the decay time axis (in Fig. 5), the fit is repeated assuming an exponential distribution with $\tau = 1.80$ ps. Bias due to the small signal size has been studied using pseudoexperiments, and we find a small fit bias in $\tau_{\Omega_b^-}/\tau_{\Xi_b^-}$, which pulls the value down by 10% of the statistical uncertainty. We correct the data for this bias, and assign half the shift as a systematic uncertainty. The simulated samples used to determine the relative efficiency are of finite size, and those

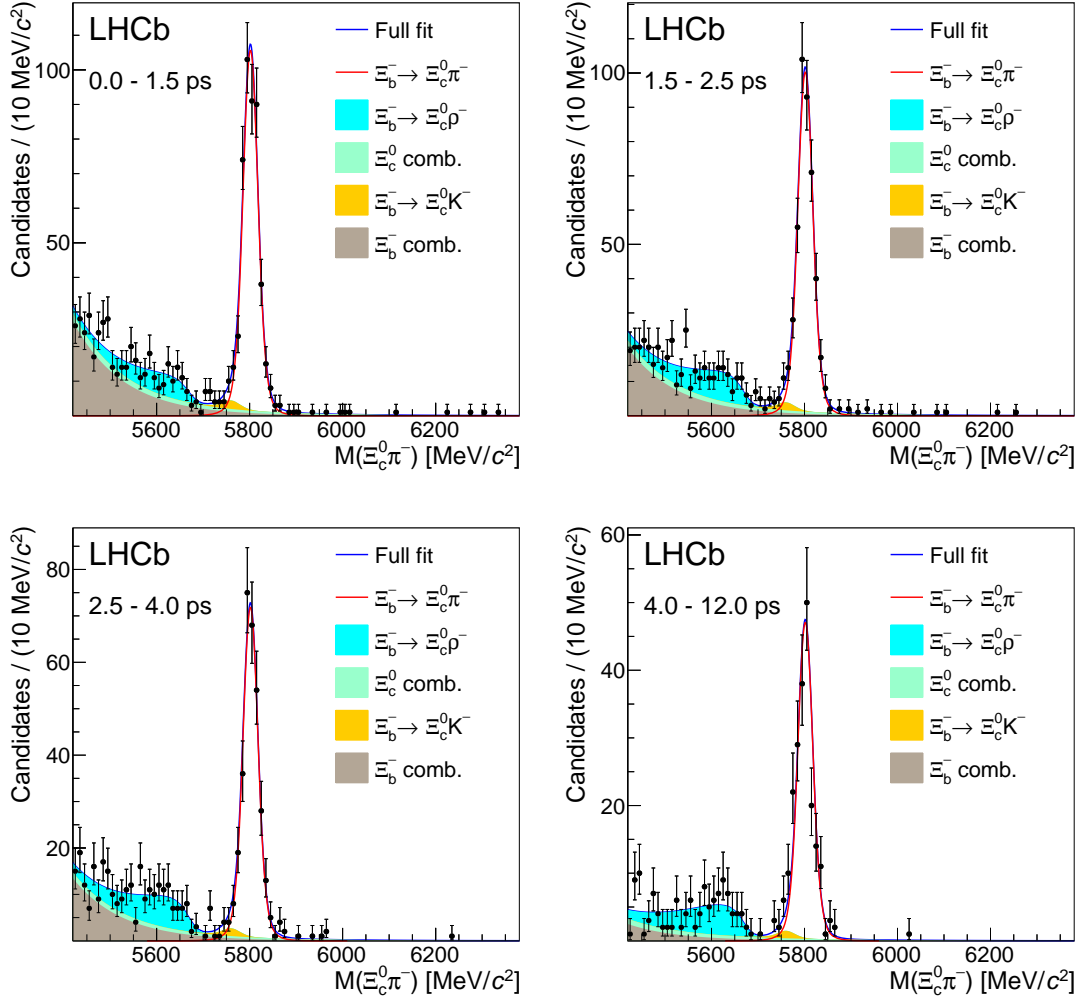


Figure 4: Results of the simultaneous mass fit to the Ξ_b^- signal in the four decay time bins, as indicated in each plot.

uncertainties are propagated to the final result.

For the δm measurement, the fitted value of $\delta m_{\text{meas}} - \delta m_{\text{true}}$ in simulation is $-0.38 \pm 0.28 \text{ MeV}/c^2$. We apply this value as a correction, and assign the $0.28 \text{ MeV}/c^2$ as a systematic uncertainty. The momentum scale has a fractional uncertainty of ± 0.0003 [40]. Its effect is evaluated by shifting all momentum components of the final-state particles by this amount in simulated decays, and comparing to the case when no shift is applied. Lastly, the uncertainty in the Ξ_b^- lifetime enters weakly into the lifetime ratio (see Eq. 5), and is also included as a source of uncertainty. All sources of systematic uncertainty are added in quadrature to obtain the corrections and systematic uncertainties of $-0.4 \pm 0.5 \text{ MeV}/c^2$ on δm and $+0.016 \pm 0.029$ on $\tau_{\Omega_b^-}/\tau_{\Xi_b^-}$.

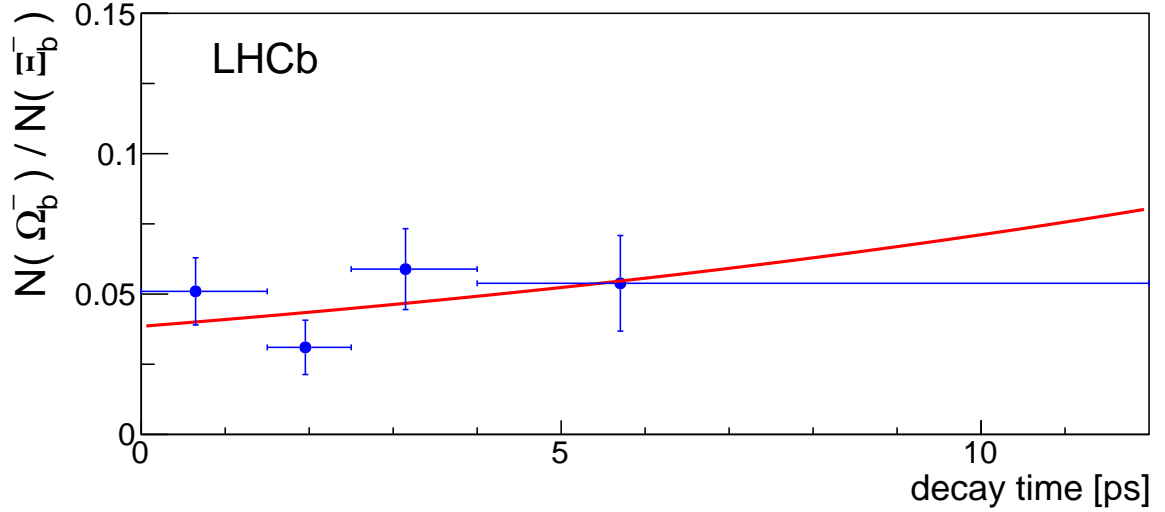


Figure 5: Corrected signal yield ratio as a function of decay time, along with a fit to an exponential function. The horizontal bars indicate the bin sizes, and are not an indication of the uncertainty.

Table 2: Summary of systematic uncertainties in δm and the lifetime ratio. When two values are indicated, the first is a correction, and the second is the uncertainty.

Source	δm (MeV/ c^2)	$\tau_{\Omega_b^-} / \tau_{\Xi_b^-}$
Signal shape	± 0.3	± 0.005
Background shape	± 0.1	± 0.009
Ω_c^{*0} shape	± 0.1	± 0.003
$X_b \rightarrow X_c K^-$ background	± 0.2	± 0.002
Relative efficiency	–	± 0.018
Average time in bin	–	± 0.002
Lifetime fit	–	$+0.016 \pm 0.008$
Simulated sample size	-0.38 ± 0.28	± 0.017
Momentum scale	± 0.1	–
Ξ_b^- lifetime	–	± 0.004
Total systematic	-0.4 ± 0.5	$+0.016 \pm 0.029$
Total statistical	± 3.2	± 0.16

7 Summary

In summary, a 3.0 fb^{-1} pp collision data sample is used to reconstruct a sample of 63 ± 9 $\Omega_b^- \rightarrow \Omega_c^0 \pi^-$, $\Omega_c^0 \rightarrow p K^- K^- \pi^+$ decays. This is the first observation of these Ω_b^- and Ω_c^0 decay modes, with well over 5σ significance. Using these signals, the mass difference and

mass are measured to be

$$\begin{aligned} m_{\Omega_b^-} - m_{\Xi_b^-} &= 247.3 \pm 3.2 \pm 0.5 \text{ MeV}/c^2, \\ m_{\Omega_b^-} &= 6045.1 \pm 3.2 \pm 0.5 \pm 0.6 \text{ MeV}/c^2, \end{aligned}$$

where the uncertainties are statistical, systematic, and from knowledge of the Ξ_b^- mass [12] ($m_{\Omega_b^-}$ only). The measured Ω_b^- mass is consistent with previous measurements from LHCb, $6046.0 \pm 2.2 \pm 0.5 \text{ MeV}/c^2$ [18], and CDF, $6047.5 \pm 3.8 \pm 0.6 \text{ MeV}/c^2$ [19], but inconsistent with the value of $6165 \pm 10 \pm 13 \text{ MeV}/c^2$ obtained by the D0 experiment [20]. An average of the two LHCb measurements yields $m_{\Omega_b^-} = 6045.7 \pm 1.9 \text{ MeV}/c^2$, where the momentum scale uncertainty is taken as 100% correlated, and the rest of the uncertainties are uncorrelated.

The lifetime ratio and absolute lifetime of the Ω_b^- baryon are also measured to be

$$\begin{aligned} \frac{\tau_{\Omega_b^-}}{\tau_{\Xi_b^-}} &= 1.11 \pm 0.16 \pm 0.03, \\ \tau_{\Omega_b^-} &= 1.78 \pm 0.26 \pm 0.05 \pm 0.06 \text{ ps}, \end{aligned}$$

using $\tau_{\Xi_b^-} = 1.599 \pm 0.041 \pm 0.022 \text{ ps}$ [12]. The first uncertainty in each case is statistical. The second uncertainty on $\tau_{\Omega_b^-}/\tau_{\Xi_b^-}$ is the total systematic uncertainty, as given in Table 2. For $\tau_{\Omega_b^-}$, the second uncertainty is from all sources in Table 2 except the Ξ_b^- lifetime, and the third uncertainty stems from the uncertainty in the Ξ_b^- lifetime. The lifetime is consistent with the previous measurements of $\tau_{\Omega_b^-} = 1.54_{-0.21}^{+0.26} \pm 0.05 \text{ ps}$ [10] and $\tau_{\Omega_b^-} = 1.66_{-0.40}^{+0.53} \text{ ps}$ [19] by the LHCb and CDF collaborations, respectively. The average of the LHCb measurements, assuming no correlation among the uncertainties, yields an Ω_b^- lifetime of $1.66_{-0.18}^{+0.19} \text{ ps}$. These measurements improve our knowledge of the mass and the lifetime of the Ω_b^- baryon. Due to the similarity of the signal and calibration modes, this pair of decay modes is very promising for future studies of the Ω_b^- baryon.

Acknowledgements

We express our gratitude to our colleagues in the CERN accelerator departments for the excellent performance of the LHC. We thank the technical and administrative staff at the LHCb institutes. We acknowledge support from CERN and from the national agencies: CAPES, CNPq, FAPERJ and FINEP (Brazil); NSFC (China); CNRS/IN2P3 (France); BMBF, DFG and MPG (Germany); INFN (Italy); FOM and NWO (The Netherlands); MNiSW and NCN (Poland); MEN/IFA (Romania); MinES and FANO (Russia); MinECo (Spain); SNSF and SER (Switzerland); NASU (Ukraine); STFC (United Kingdom); NSF (USA). We acknowledge the computing resources that are provided by CERN, IN2P3 (France), KIT and DESY (Germany), INFN (Italy), SURF (The Netherlands), PIC (Spain), GridPP (United Kingdom), RRCKI and Yandex LLC (Russia), CSCS (Switzerland), IFIN-HH (Romania), CBPF (Brazil), PL-GRID (Poland) and OSC (USA). We are indebted to the communities behind the multiple open source software packages on which we depend. Individual groups or members have received support from AvH Foundation (Germany),

EPLANET, Marie Skłodowska-Curie Actions and ERC (European Union), Conseil Général de Haute-Savoie, Labex ENIGMASS and OCEVU, Région Auvergne (France), RFBR and Yandex LLC (Russia), GVA, XuntaGal and GENCAT (Spain), Herchel Smith Fund, The Royal Society, Royal Commission for the Exhibition of 1851 and the Leverhulme Trust (United Kingdom).

References

- [1] V. A. Khoze and M. A. Shifman, *Heavy quarks*, Sov. Phys. Usp. **26** (1983) 387.
- [2] I. I. Bigi and N. G. Uraltsev, *Gluonic enhancements in non-spectator beauty decays – an inclusive mirage though an exclusive possibility*, Phys. Lett. **B280** (1992) 271.
- [3] I. I. Bigi, N. G. Uraltsev, and A. I. Vainshtein, *Nonperturbative corrections to inclusive beauty and charm decays: QCD versus phenomenological models*, Phys. Lett. **B293** (1992) 430, Erratum ibid. **B297** (1992) 477, arXiv:hep-ph/9207214.
- [4] B. Blok and M. Shifman, *The rule of discarding $1/N_c$ in inclusive weak decays (I)*, Nucl. Phys. **B399** (1993) 441, arXiv:hep-ph/9207236.
- [5] B. Blok and M. Shifman, *The rule of discarding $1/N_c$ in inclusive weak decays (II)*, Nucl. Phys. **B399** (1993) 459, arXiv:hep-ph/9209289.
- [6] M. Neubert, *B decays and the heavy quark expansion*, Adv. Ser. Direct. High Energy Phys. **15** (1998) 239, arXiv:hep-ph/9702375.
- [7] N. Uraltsev, *Heavy quark expansion in beauty and its decays*, arXiv:hep-ph/9804275.
- [8] G. Bellini, I. I. Y. Bigi, and P. J. Dornan, *Lifetimes of charm and beauty hadrons*, Phys. Rep. **289** (1997) 1.
- [9] LHCb collaboration, R. Aaij *et al.*, *Precision measurement of the ratio of the Λ_b^0 to \bar{B}^0 lifetimes*, Phys. Lett. **B734** (2014) 122, arXiv:1402.6242.
- [10] LHCb collaboration, R. Aaij *et al.*, *Measurement of the Ξ_b^- and Ω_b^- baryon lifetimes*, Phys. Lett. **B736** (2014) 154, arXiv:1405.1543.
- [11] LHCb collaboration, R. Aaij *et al.*, *Precision measurement of the mass and lifetime of the Ξ_b^0 baryon*, Phys. Rev. Lett. **113** (2014) 032001, arXiv:1405.7223.
- [12] LHCb collaboration, R. Aaij *et al.*, *Precision measurement of the mass and lifetime of the Ξ_b^- baryon*, Phys. Rev. Lett. **113** (2014) 242002, arXiv:1409.8568.
- [13] Particle Data Group, K. A. Olive *et al.*, *Review of particle physics*, Chin. Phys. **C38** (2014) 090001, and 2015 update.
- [14] I. I. Y. Bigi, *The QCD perspective on lifetimes of heavy flavor hadrons*, arXiv:hep-ph/9508408.
- [15] H.-Y. Cheng, *A phenomenological analysis of heavy hadron lifetimes*, Phys. Rev. **D56** (1997) 2783, arXiv:hep-ph/9704260.
- [16] T. Ito, M. Matsuda, and Y. Matsui, *New possibility of solving the problem of lifetime ratio $\tau(\Lambda_b^0)/\tau(B_d)$* , Prog. Theor. Phys. **99** (1998) 271, arXiv:hep-ph/9705402.

- [17] C. Amsler, T. Degrand and B. Krusche, *Quark model*, published in Ref. [13].
- [18] LHCb collaboration, R. Aaij *et al.*, *Measurements of the Λ_b^0 , Ξ_b^- , and Ω_b^- baryon masses*, Phys. Rev. Lett. **110** (2013) 182001, [arXiv:1302.1072](#).
- [19] CDF collaboration, T. A. Aaltonen *et al.*, *Mass and lifetime measurements of bottom and charm baryons in $p\bar{p}$ collisions at $\sqrt{s} = 1.96$ TeV*, Phys. Rev. **D89** (2014) 072014, [arXiv:1403.8126](#).
- [20] D0 collaboration, V. M. Abazov *et al.*, *Observation of the doubly strange b baryon Ω_b^-* , Phys. Rev. Lett. **101** (2008) 232002, [arXiv:0808.4142](#).
- [21] LHCb collaboration, A. A. Alves Jr. *et al.*, *The LHCb detector at the LHC*, JINST **3** (2008) S08005.
- [22] LHCb collaboration, R. Aaij *et al.*, *LHCb detector performance*, Int. J. Mod. Phys. **A30** (2015) 1530022, [arXiv:1412.6352](#).
- [23] R. Aaij *et al.*, *The LHCb trigger and its performance in 2011*, JINST **8** (2013) P04022, [arXiv:1211.3055](#).
- [24] V. V. Gligorov and M. Williams, *Efficient, reliable and fast high-level triggering using a bonsai boosted decision tree*, JINST **8** (2013) P02013, [arXiv:1210.6861](#).
- [25] T. Sjöstrand, S. Mrenna, and P. Skands, *PYTHIA 6.4 physics and manual*, JHEP **05** (2006) 026, [arXiv:hep-ph/0603175](#); T. Sjöstrand, S. Mrenna, and P. Skands, *A brief introduction to PYTHIA 8.1*, Comput. Phys. Commun. **178** (2008) 852, [arXiv:0710.3820](#).
- [26] I. Belyaev *et al.*, *Handling of the generation of primary events in Gauss, the LHCb simulation framework*, J. Phys. Conf. Ser. **331** (2011) 032047.
- [27] D. J. Lange, *The EvtGen particle decay simulation package*, Nucl. Instrum. Meth. **A462** (2001) 152.
- [28] P. Golonka and Z. Was, *PHOTOS Monte Carlo: A precision tool for QED corrections in Z and W decays*, Eur. Phys. J. **C45** (2006) 97, [arXiv:hep-ph/0506026](#).
- [29] Geant4 collaboration, J. Allison *et al.*, *Geant4 developments and applications*, IEEE Trans. Nucl. Sci. **53** (2006) 270; Geant4 collaboration, S. Agostinelli *et al.*, *Geant4: A simulation toolkit*, Nucl. Instrum. Meth. **A506** (2003) 250.
- [30] M. Clemencic *et al.*, *The LHCb simulation application, Gauss: Design, evolution and experience*, J. Phys. Conf. Ser. **331** (2011) 032023.
- [31] L. Breiman, J. H. Friedman, R. A. Olshen, and C. J. Stone, *Classification and regression trees*, Wadsworth international group, Belmont, California, USA, 1984.

- [32] R. E. Schapire and Y. Freund, *A decision-theoretic generalization of on-line learning and an application to boosting*, Jour. Comp. and Syst. Sc. **55** (1997) 119.
- [33] A. Hoecker *et al.*, *TMVA: Toolkit for multivariate data analysis*, PoS **ACAT** (2007) 040, [arXiv:physics/0703039](https://arxiv.org/abs/physics/0703039).
- [34] M. Adinolfi *et al.*, *Performance of the LHCb RICH detector at the LHC*, Eur. Phys. J. **C73** (2013) 2431, [arXiv:1211.6759](https://arxiv.org/abs/1211.6759).
- [35] T. Skwarnicki, *A study of the radiative cascade transitions between the Upsilon-prime and Upsilon resonances*, PhD thesis, Institute of Nuclear Physics, Krakow, 1986, DESY-F31-86-02.
- [36] ARGUS collaboration, H. Albrecht *et al.*, *Measurement of the polarization in the decay $B \rightarrow J/\psi K^*$* , Phys. Lett. **B340** (1994) 217.
- [37] LHCb collaboration, R. Aaij *et al.*, *Study of beauty baryon decays to $D^0 p h^-$ and $\Lambda_c^+ h^-$ final states*, Phys. Rev. **D89** (2014) 032001, [arXiv:1311.4823](https://arxiv.org/abs/1311.4823).
- [38] R. Brun and F. Rademakers, *ROOT: An object oriented data analysis framework*, Nucl. Instrum. Meth. **A389** (1997) 81, see <https://root.cern.ch/doc/master/classTGenPhaseSpace.html> for additional details.
- [39] S. S. Wilks, *The large-sample distribution of the likelihood ratio for testing composite hypotheses*, Annals Math. Statist. **9** (1938) 60.
- [40] LHCb collaboration, R. Aaij *et al.*, *Precision measurement of D meson mass differences*, JHEP **06** (2013) 065, [arXiv:1304.6865](https://arxiv.org/abs/1304.6865).

LHCb collaboration

R. Aaij³⁹, C. Abellán Beteta⁴¹, B. Adeva³⁸, M. Adinolfi⁴⁷, Z. Ajaltouni⁵, S. Akar⁶, J. Albrecht¹⁰, F. Alessio³⁹, M. Alexander⁵², S. Ali⁴², G. Alkhazov³¹, P. Alvarez Cartelle⁵⁴, A.A. Alves Jr⁵⁸, S. Amato², S. Amerio²³, Y. Amhis⁷, L. An^{3,40}, L. Anderlini¹⁸, G. Andreassi⁴⁰, M. Andreotti^{17,g}, J.E. Andrews⁵⁹, R.B. Appleby⁵⁵, O. Aquines Gutierrez¹¹, F. Archilli³⁹, P. d'Argent¹², A. Artamonov³⁶, M. Artuso⁶⁰, E. Aslanides⁶, G. Auriemma^{26,n}, M. Baalouch⁵, S. Bachmann¹², J.J. Back⁴⁹, A. Badalov³⁷, C. Baesso⁶¹, S. Baker⁵⁴, W. Baldini¹⁷, R.J. Barlow⁵⁵, C. Barschel³⁹, S. Barsuk⁷, W. Barter³⁹, V. Batozskaya²⁹, V. Battista⁴⁰, A. Bay⁴⁰, L. Beaucourt⁴, J. Beddow⁵², F. Bedeschi²⁴, I. Bediaga¹, L.J. Bel⁴², V. Bellec⁴⁰, N. Belloli^{21,k}, I. Belyaev³², E. Ben-Haim⁸, G. Bencivenni¹⁹, S. Benson³⁹, J. Benton⁴⁷, A. Berezhnoy³³, R. Bernet⁴¹, A. Bertolin²³, F. Betti¹⁵, M.-O. Bettler³⁹, M. van Beuzekom⁴², S. Bifani⁴⁶, P. Billoir⁸, T. Bird⁵⁵, A. Birnkraut¹⁰, A. Bizzeti^{18,i}, T. Blake⁴⁹, F. Blanc⁴⁰, J. Blouw¹¹, S. Blusk⁶⁰, V. Bocci²⁶, A. Bondar³⁵, N. Bondar^{31,39}, W. Bonivento¹⁶, A. Borgheresi^{21,k}, S. Borghi⁵⁵, M. Borisyak⁶⁷, M. Borsato³⁸, M. Boubdir⁹, T.J.V. Bowcock⁵³, E. Bowen⁴¹, C. Bozzi^{17,39}, S. Braun¹², M. Britsch¹², T. Britton⁶⁰, J. Brodzicka⁵⁵, E. Buchanan⁴⁷, C. Burr⁵⁵, A. Bursche², J. Buytaert³⁹, S. Cadeddu¹⁶, R. Calabrese^{17,g}, M. Calvi^{21,k}, M. Calvo Gomez^{37,p}, P. Campana¹⁹, D. Campora Perez³⁹, L. Capriotti⁵⁵, A. Carbone^{15,e}, G. Carboni^{25,l}, R. Cardinale^{20,j}, A. Cardini¹⁶, P. Carniti^{21,k}, L. Carson⁵¹, K. Carvalho Akiba², G. Casse⁵³, L. Cassina^{21,k}, L. Castillo Garcia⁴⁰, M. Cattaneo³⁹, Ch. Cauet¹⁰, G. Cavallero²⁰, R. Cenci^{24,t}, M. Charles⁸, Ph. Charpentier³⁹, G. Chatzikonstantinidis⁴⁶, M. Chefdeville⁴, S. Chen⁵⁵, S.-F. Cheung⁵⁶, V. Chobanova³⁸, M. Chrzaszcz^{41,27}, X. Cid Vidal³⁹, G. Ciezarek⁴², P.E.L. Clarke⁵¹, M. Clemencic³⁹, H.V. Cliff⁴⁸, J. Closier³⁹, V. Coco⁵⁸, J. Cogan⁶, E. Cogneras⁵, V. Cogoni^{16,f}, L. Cojocariu³⁰, G. Collazuol^{23,r}, P. Collins³⁹, A. Comerma-Montells¹², A. Contu³⁹, A. Cook⁴⁷, S. Coquereau⁸, G. Corti³⁹, M. Corvo^{17,g}, B. Couturier³⁹, G.A. Cowan⁵¹, D.C. Craik⁵¹, A. Crocombe⁴⁹, M. Cruz Torres⁶¹, S. Cunliffe⁵⁴, R. Currie⁵⁴, C. D'Ambrosio³⁹, E. Dall'Occo⁴², J. Dalseno⁴⁷, P.N.Y. David⁴², A. Davis⁵⁸, O. De Aguiar Francisco², K. De Bruyn⁶, S. De Capua⁵⁵, M. De Cian¹², J.M. De Miranda¹, L. De Paula², P. De Simone¹⁹, C.-T. Dean⁵², D. Decamp⁴, M. Deckenhoff¹⁰, L. Del Buono⁸, N. Déleage⁴, M. Demmer¹⁰, D. Derkach⁶⁷, O. Deschamps⁵, F. Dettori³⁹, B. Dey²², A. Di Canto³⁹, H. Dijkstra³⁹, F. Dordei³⁹, M. Dorigo⁴⁰, A. Dosil Suárez³⁸, A. Dovbnya⁴⁴, K. Dreimanis⁵³, L. Dufour⁴², G. Dujany⁵⁵, K. Dungs³⁹, P. Durante³⁹, R. Dzhelyadin³⁶, A. Dziurda²⁷, A. Dzyuba³¹, S. Easo^{50,39}, U. Egede⁵⁴, V. Egorychev³², S. Eidelman³⁵, S. Eisenhardt⁵¹, U. Eitschberger¹⁰, R. Ekelhof¹⁰, L. Eklund⁵², I. El Rifai⁵, Ch. Elsasser⁴¹, S. Ely⁶⁰, S. Esen¹², H.M. Evans⁴⁸, T. Evans⁵⁶, A. Falabella¹⁵, C. Färber³⁹, N. Farley⁴⁶, S. Farry⁵³, R. Fay⁵³, D. Fazzini^{21,k}, D. Ferguson⁵¹, V. Fernandez Albor³⁸, F. Ferrari¹⁵, F. Ferreira Rodrigues¹, M. Ferro-Luzzi³⁹, S. Filippov³⁴, M. Fiore^{17,g}, M. Fiorini^{17,g}, M. Firlej²⁸, C. Fitzpatrick⁴⁰, T. Fiutowski²⁸, F. Fleuret^{7,b}, K. Fohl³⁹, M. Fontana¹⁶, F. Fontanelli^{20,j}, D. C. Forshaw⁶⁰, R. Forty³⁹, M. Frank³⁹, C. Frei³⁹, M. Frosini¹⁸, J. Fu²², E. Furfaro^{25,l}, A. Gallas Torreira³⁸, D. Galli^{15,e}, S. Gallorini²³, S. Gambetta⁵¹, M. Gandelman², P. Gandini⁵⁶, Y. Gao³, J. García Pardiñas³⁸, J. Garra Tico⁴⁸, L. Garrido³⁷, P.J. Garsed⁴⁸, D. Gascon³⁷, C. Gaspar³⁹, L. Gavardi¹⁰, G. Gazzoni⁵, D. Gerick¹², E. Gersabeck¹², M. Gersabeck⁵⁵, T. Gershon⁴⁹, Ph. Ghez⁴, S. Gianì⁴⁰, V. Gibson⁴⁸, O.G. Girard⁴⁰, L. Giubega³⁰, V.V. Gligorov³⁹, C. Göbel⁶¹, D. Golubkov³², A. Golutvin^{54,39}, A. Gomes^{1,a}, C. Gotti^{21,k}, M. Grabalosa Gándara⁵, R. Graciani Diaz³⁷, L.A. Granado Cardoso³⁹, E. Graugés³⁷, E. Graverini⁴¹, G. Graziani¹⁸, A. Grecu³⁰, P. Griffith⁴⁶, L. Grillo¹², O. Grünberg⁶⁵, E. Gushchin³⁴, Yu. Guz^{36,39}, T. Gys³⁹, T. Hadavizadeh⁵⁶,

C. Hadjivasiliou⁶⁰, G. Haefeli⁴⁰, C. Haen³⁹, S.C. Haines⁴⁸, S. Hall⁵⁴, B. Hamilton⁵⁹, X. Han¹²,
 S. Hansmann-Menzemer¹², N. Harnew⁵⁶, S.T. Harnew⁴⁷, J. Harrison⁵⁵, J. He³⁹, T. Head⁴⁰,
 A. Heister⁹, K. Hennessy⁵³, P. Henrard⁵, L. Henry⁸, J.A. Hernando Morata³⁸,
 E. van Herwijnen³⁹, M. Heß⁶⁵, A. Hicheur², D. Hill⁵⁶, M. Hoballah⁵, C. Hombach⁵⁵,
 L. Hongming⁴⁰, W. Hulsbergen⁴², T. Humair⁵⁴, M. Hushchyn⁶⁷, N. Hussain⁵⁶, D. Hutchcroft⁵³,
 M. Idzik²⁸, P. Ilten⁵⁷, R. Jacobsson³⁹, A. Jaeger¹², J. Jalocha⁵⁶, E. Jans⁴², A. Jawahery⁵⁹,
 M. John⁵⁶, D. Johnson³⁹, C.R. Jones⁴⁸, C. Joram³⁹, B. Jost³⁹, N. Jurik⁶⁰, S. Kandybei⁴⁴,
 W. Kanso⁶, M. Karacson³⁹, T.M. Karbach^{39,†}, S. Karodia⁵², M. Kecke¹², M. Kelsey⁶⁰,
 I.R. Kenyon⁴⁶, M. Kenzie³⁹, T. Ketel⁴³, E. Khairullin⁶⁷, B. Khanji^{21,39,k}, C. Khurewathanakul⁴⁰,
 T. Kirn⁹, S. Klaver⁵⁵, K. Klimaszewski²⁹, M. Kolpin¹², I. Komarov⁴⁰, R.F. Koopman⁴³,
 P. Koppenburg⁴², M. Kozeiha⁵, L. Kravchuk³⁴, K. Kreplin¹², M. Kreps⁴⁹, P. Krokovny³⁵,
 F. Kruse¹⁰, W. Krzemien²⁹, W. Kucewicz^{27,o}, M. Kucharczyk²⁷, V. Kudryavtsev³⁵, A.
 K. Kuonen⁴⁰, K. Kurek²⁹, T. Kvaratskheliya³², D. Lacarrere³⁹, G. Lafferty^{55,39}, A. Lai¹⁶,
 D. Lambert⁵¹, G. Lanfranchi¹⁹, C. Langenbruch⁴⁹, B. Langhans³⁹, T. Latham⁴⁹, C. Lazzeroni⁴⁶,
 R. Le Gac⁶, J. van Leerdam⁴², J.-P. Lees⁴, R. Lefèvre⁵, A. Leflat^{33,39}, J. Lefrançois⁷,
 E. Lemos Cid³⁸, O. Leroy⁶, T. Lesiak²⁷, B. Leverington¹², Y. Li⁷, T. Likhomanenko^{67,66},
 R. Lindner³⁹, C. Linn³⁹, F. Lionetto⁴¹, B. Liu¹⁶, X. Liu³, D. Loh⁴⁹, I. Longstaff⁵², J.H. Lopes²,
 D. Lucchesi^{23,r}, M. Lucio Martinez³⁸, H. Luo⁵¹, A. Lupato²³, E. Luppi^{17,g}, O. Lupton⁵⁶,
 N. Lusardi²², A. Lusiani²⁴, X. Lyu⁶², F. Machefert⁷, F. Maciuc³⁰, O. Maev³¹, K. Maguire⁵⁵,
 S. Malde⁵⁶, A. Malinin⁶⁶, G. Manca⁷, G. Mancinelli⁶, P. Manning⁶⁰, A. Mapelli³⁹, J. Maratas⁵,
 J.F. Marchand⁴, U. Marconi¹⁵, C. Marin Benito³⁷, P. Marino^{24,t}, J. Marks¹², G. Martellotti²⁶,
 M. Martin⁶, M. Martinelli⁴⁰, D. Martinez Santos³⁸, F. Martinez Vidal⁶⁸, D. Martins Tostes²,
 L.M. Massacrier⁷, A. Massafferri¹, R. Matev³⁹, A. Mathad⁴⁹, Z. Mathe³⁹, C. Matteuzzi²¹,
 A. Mauri⁴¹, B. Maurin⁴⁰, A. Mazurov⁴⁶, M. McCann⁵⁴, J. McCarthy⁴⁶, A. McNab⁵⁵,
 R. McNulty¹³, B. Meadows⁵⁸, F. Meier¹⁰, M. Meissner¹², D. Melnychuk²⁹, M. Merk⁴²,
 A Merli^{22,u}, E. Michielin²³, D.A. Milanese⁶⁴, M.-N. Minard⁴, D.S. Mitzel¹²,
 J. Molina Rodriguez⁶¹, I.A. Monroy⁶⁴, S. Monteil⁵, M. Morandin²³, P. Morawski²⁸, A. Mordà⁶,
 M.J. Morello^{24,t}, J. Moron²⁸, A.B. Morris⁵¹, R. Mountain⁶⁰, F. Muheim⁵¹, D. Müller⁵⁵,
 J. Müller¹⁰, K. Müller⁴¹, V. Müller¹⁰, M. Mussini¹⁵, B. Muster⁴⁰, P. Naik⁴⁷, T. Nakada⁴⁰,
 R. Nandakumar⁵⁰, A. Nandi⁵⁶, I. Nasteva², M. Needham⁵¹, N. Neri²², S. Neubert¹²,
 N. Neufeld³⁹, M. Neuner¹², A.D. Nguyen⁴⁰, C. Nguyen-Mau^{40,q}, V. Niess⁵, S. Nieswand⁹,
 R. Niet¹⁰, N. Nikitin³³, T. Nikodem¹², A. Novoselov³⁶, D.P. O’Hanlon⁴⁹,
 A. Oblakowska-Mucha²⁸, V. Obraztsov³⁶, S. Ogilvy⁵², O. Okhrimenko⁴⁵, R. Oldeman^{16,48,f},
 C.J.G. Onderwater⁶⁹, B. Osorio Rodrigues¹, J.M. Otalora Goicochea², A. Otto³⁹, P. Owen⁵⁴,
 A. Oyanguren⁶⁸, A. Palano^{14,d}, F. Palombo^{22,u}, M. Palutan¹⁹, J. Panman³⁹, A. Papanestis⁵⁰,
 M. Pappagallo⁵², L.L. Pappalardo^{17,g}, C. Pappenheimer⁵⁸, W. Parker⁵⁹, C. Parkes⁵⁵,
 G. Passaleva¹⁸, G.D. Patel⁵³, M. Patel⁵⁴, C. Patrignani^{20,j}, A. Pearce^{55,50}, A. Pellegrino⁴²,
 G. Penso^{26,m}, M. Pepe Altarelli³⁹, S. Perazzini^{15,e}, P. Perret⁵, L. Pescatore⁴⁶, K. Petridis⁴⁷,
 A. Petrolini^{20,j}, M. Petruzzo²², E. Picatoste Olloqui³⁷, B. Pietrzyk⁴, M. Piekies²⁷, D. Pinci²⁶,
 A. Pistone²⁰, A. Piucci¹², S. Playfer⁵¹, M. Plo Casasus³⁸, T. Poikela³⁹, F. Polci⁸,
 A. Poluektov^{49,35}, I. Polyakov³², E. Polcarpo², A. Popov³⁶, D. Popov^{11,39}, B. Popovici³⁰,
 C. Potterat², E. Price⁴⁷, J.D. Price⁵³, J. Prisciandaro³⁸, A. Pritchard⁵³, C. Prouve⁴⁷,
 V. Pugatch⁴⁵, A. Puig Navarro⁴⁰, G. Punzi^{24,s}, W. Qian⁵⁶, R. Quagliani^{7,47}, B. Rachwal²⁷,
 J.H. Rademacker⁴⁷, M. Rama²⁴, M. Ramos Pernas³⁸, M.S. Rangel², I. Raniuk⁴⁴, G. Raven⁴³,
 F. Redi⁵⁴, S. Reichert¹⁰, A.C. dos Reis¹, V. Renaudin⁷, S. Ricciardi⁵⁰, S. Richards⁴⁷, M. Rihl³⁹,
 K. Rinnert^{53,39}, V. Rives Molina³⁷, P. Robbe⁷, A.B. Rodrigues¹, E. Rodrigues⁵⁸,

J.A. Rodriguez Lopez⁶⁴, P. Rodriguez Perez⁵⁵, A. Rogozhnikov⁶⁷, S. Roiser³⁹, V. Romanovsky³⁶, A. Romero Vidal³⁸, J. W. Ronayne¹³, M. Rotondo²³, T. Ruf³⁹, P. Ruiz Valls⁶⁸, J.J. Saborido Silva³⁸, N. Sagidova³¹, B. Saitta^{16,f}, V. Salustino Guimaraes², C. Sanchez Mayordomo⁶⁸, B. Sanmartin Sedes³⁸, R. Santacesaria²⁶, C. Santamarina Rios³⁸, M. Santimaria¹⁹, E. Santovetti^{25,l}, A. Sarti^{19,m}, C. Satriano^{26,n}, A. Satta²⁵, D.M. Saunders⁴⁷, D. Savrina^{32,33}, S. Schael⁹, M. Schiller³⁹, H. Schindler³⁹, M. Schlupp¹⁰, M. Schmelling¹¹, T. Schmelzer¹⁰, B. Schmidt³⁹, O. Schneider⁴⁰, A. Schopper³⁹, M. Schubiger⁴⁰, M.-H. Schune⁷, R. Schwemmer³⁹, B. Sciascia¹⁹, A. Sciubba^{26,m}, A. Semennikov³², A. Sergi⁴⁶, N. Serra⁴¹, J. Serrano⁶, L. Sestini²³, P. Seyfert²¹, M. Shapkin³⁶, I. Shapoval^{17,44,g}, Y. Shcheglov³¹, T. Shears⁵³, L. Shekhtman³⁵, V. Shevchenko⁶⁶, A. Shires¹⁰, B.G. Siddi¹⁷, R. Silva Coutinho⁴¹, L. Silva de Oliveira², G. Simi^{23,s}, M. Sirendi⁴⁸, N. Skidmore⁴⁷, T. Skwarnicki⁶⁰, E. Smith⁵⁴, I.T. Smith⁵¹, J. Smith⁴⁸, M. Smith⁵⁵, H. Snoek⁴², M.D. Sokoloff⁵⁸, F.J.P. Soler⁵², F. Soomro⁴⁰, D. Souza⁴⁷, B. Souza De Paula², B. Spaan¹⁰, P. Spradlin⁵², S. Sridharan³⁹, F. Stagni³⁹, M. Stahl¹², S. Stahl³⁹, S. Stefkova⁵⁴, O. Steinkamp⁴¹, O. Stenyakin³⁶, S. Stevenson⁵⁶, S. Stoica³⁰, S. Stone⁶⁰, B. Storaci⁴¹, S. Stracka^{24,t}, M. Straticiu³⁰, U. Straumann⁴¹, L. Sun⁵⁸, W. Sutcliffe⁵⁴, K. Swientek²⁸, S. Swientek¹⁰, V. Syropoulos⁴³, M. Szczekowski²⁹, T. Szumlak²⁸, S. T'Jampens⁴, A. Tayduganov⁶, T. Tekampe¹⁰, G. Tellarini^{17,g}, F. Teubert³⁹, C. Thomas⁵⁶, E. Thomas³⁹, J. van Tilburg⁴², V. Tisserand⁴, M. Tobin⁴⁰, S. Tolk⁴³, L. Tomassetti^{17,g}, D. Tonelli³⁹, S. Topp-Joergensen⁵⁶, E. Tournefier⁴, S. Tourneur⁴⁰, K. Trabelsi⁴⁰, M. Traill⁵², M.T. Tran⁴⁰, M. Tresch⁴¹, A. Trisovic³⁹, A. Tsaregorodtsev⁶, P. Tsopelas⁴², N. Tuning^{42,39}, A. Ukleja²⁹, A. Ustyuzhanin^{67,66}, U. Uwer¹², C. Vacca^{16,39,f}, V. Vagnoni^{15,39}, S. Valat³⁹, G. Valenti¹⁵, A. Vallier⁷, R. Vazquez Gomez¹⁹, P. Vazquez Regueiro³⁸, C. Vázquez Sierra³⁸, S. Vecchi¹⁷, M. van Veghel⁴², J.J. Velthuis⁴⁷, M. Veltri^{18,h}, G. Veneziano⁴⁰, M. Vesterinen¹², B. Viaud⁷, D. Vieira², M. Vieites Diaz³⁸, X. Vilasis-Cardona^{37,p}, V. Volkov³³, A. Vollhardt⁴¹, D. Voong⁴⁷, A. Vorobyev³¹, V. Vorobyev³⁵, C. Voß⁶⁵, J.A. de Vries⁴², R. Waldi⁶⁵, C. Wallace⁴⁹, R. Wallace¹³, J. Walsh²⁴, J. Wang⁶⁰, D.R. Ward⁴⁸, N.K. Watson⁴⁶, D. Websdale⁵⁴, A. Weiden⁴¹, M. Whitehead³⁹, J. Wicht⁴⁹, G. Wilkinson^{56,39}, M. Wilkinson⁶⁰, M. Williams³⁹, M.P. Williams⁴⁶, M. Williams⁵⁷, T. Williams⁴⁶, F.F. Wilson⁵⁰, J. Wimberley⁵⁹, J. Wishahi¹⁰, W. Wislicki²⁹, M. Witek²⁷, G. Wormser⁷, S.A. Wotton⁴⁸, K. Wraight⁵², S. Wright⁴⁸, K. Wyllie³⁹, Y. Xie⁶³, Z. Xu⁴⁰, Z. Yang³, H. Yin⁶³, J. Yu⁶³, X. Yuan³⁵, O. Yushchenko³⁶, M. Zangoli¹⁵, M. Zavertyaev^{11,c}, L. Zhang³, Y. Zhang³, A. Zhelezov¹², Y. Zheng⁶², A. Zhokhov³², L. Zhong³, V. Zhukov⁹, S. Zucchelli¹⁵.

¹Centro Brasileiro de Pesquisas Físicas (CBPF), Rio de Janeiro, Brazil

²Universidade Federal do Rio de Janeiro (UFRJ), Rio de Janeiro, Brazil

³Center for High Energy Physics, Tsinghua University, Beijing, China

⁴LAPP, Université Savoie Mont-Blanc, CNRS/IN2P3, Annecy-Le-Vieux, France

⁵Clermont Université, Université Blaise Pascal, CNRS/IN2P3, LPC, Clermont-Ferrand, France

⁶CPPM, Aix-Marseille Université, CNRS/IN2P3, Marseille, France

⁷LAL, Université Paris-Sud, CNRS/IN2P3, Orsay, France

⁸LPNHE, Université Pierre et Marie Curie, Université Paris Diderot, CNRS/IN2P3, Paris, France

⁹I. Physikalisches Institut, RWTH Aachen University, Aachen, Germany

¹⁰Fakultät Physik, Technische Universität Dortmund, Dortmund, Germany

¹¹Max-Planck-Institut für Kernphysik (MPIK), Heidelberg, Germany

¹²Physikalisches Institut, Ruprecht-Karls-Universität Heidelberg, Heidelberg, Germany

¹³School of Physics, University College Dublin, Dublin, Ireland

¹⁴Sezione INFN di Bari, Bari, Italy

¹⁵Sezione INFN di Bologna, Bologna, Italy

- ¹⁶ *Sezione INFN di Cagliari, Cagliari, Italy*
- ¹⁷ *Sezione INFN di Ferrara, Ferrara, Italy*
- ¹⁸ *Sezione INFN di Firenze, Firenze, Italy*
- ¹⁹ *Laboratori Nazionali dell'INFN di Frascati, Frascati, Italy*
- ²⁰ *Sezione INFN di Genova, Genova, Italy*
- ²¹ *Sezione INFN di Milano Bicocca, Milano, Italy*
- ²² *Sezione INFN di Milano, Milano, Italy*
- ²³ *Sezione INFN di Padova, Padova, Italy*
- ²⁴ *Sezione INFN di Pisa, Pisa, Italy*
- ²⁵ *Sezione INFN di Roma Tor Vergata, Roma, Italy*
- ²⁶ *Sezione INFN di Roma La Sapienza, Roma, Italy*
- ²⁷ *Henryk Niewodniczanski Institute of Nuclear Physics Polish Academy of Sciences, Kraków, Poland*
- ²⁸ *AGH - University of Science and Technology, Faculty of Physics and Applied Computer Science, Kraków, Poland*
- ²⁹ *National Center for Nuclear Research (NCBJ), Warsaw, Poland*
- ³⁰ *Horia Hulubei National Institute of Physics and Nuclear Engineering, Bucharest-Magurele, Romania*
- ³¹ *Petersburg Nuclear Physics Institute (PNPI), Gatchina, Russia*
- ³² *Institute of Theoretical and Experimental Physics (ITEP), Moscow, Russia*
- ³³ *Institute of Nuclear Physics, Moscow State University (SINP MSU), Moscow, Russia*
- ³⁴ *Institute for Nuclear Research of the Russian Academy of Sciences (INR RAN), Moscow, Russia*
- ³⁵ *Budker Institute of Nuclear Physics (SB RAS) and Novosibirsk State University, Novosibirsk, Russia*
- ³⁶ *Institute for High Energy Physics (IHEP), Protvino, Russia*
- ³⁷ *Universitat de Barcelona, Barcelona, Spain*
- ³⁸ *Universidad de Santiago de Compostela, Santiago de Compostela, Spain*
- ³⁹ *European Organization for Nuclear Research (CERN), Geneva, Switzerland*
- ⁴⁰ *Ecole Polytechnique Fédérale de Lausanne (EPFL), Lausanne, Switzerland*
- ⁴¹ *Physik-Institut, Universität Zürich, Zürich, Switzerland*
- ⁴² *Nikhef National Institute for Subatomic Physics, Amsterdam, The Netherlands*
- ⁴³ *Nikhef National Institute for Subatomic Physics and VU University Amsterdam, Amsterdam, The Netherlands*
- ⁴⁴ *NSC Kharkiv Institute of Physics and Technology (NSC KIPT), Kharkiv, Ukraine*
- ⁴⁵ *Institute for Nuclear Research of the National Academy of Sciences (KINR), Kyiv, Ukraine*
- ⁴⁶ *University of Birmingham, Birmingham, United Kingdom*
- ⁴⁷ *H.H. Wills Physics Laboratory, University of Bristol, Bristol, United Kingdom*
- ⁴⁸ *Cavendish Laboratory, University of Cambridge, Cambridge, United Kingdom*
- ⁴⁹ *Department of Physics, University of Warwick, Coventry, United Kingdom*
- ⁵⁰ *STFC Rutherford Appleton Laboratory, Didcot, United Kingdom*
- ⁵¹ *School of Physics and Astronomy, University of Edinburgh, Edinburgh, United Kingdom*
- ⁵² *School of Physics and Astronomy, University of Glasgow, Glasgow, United Kingdom*
- ⁵³ *Oliver Lodge Laboratory, University of Liverpool, Liverpool, United Kingdom*
- ⁵⁴ *Imperial College London, London, United Kingdom*
- ⁵⁵ *School of Physics and Astronomy, University of Manchester, Manchester, United Kingdom*
- ⁵⁶ *Department of Physics, University of Oxford, Oxford, United Kingdom*
- ⁵⁷ *Massachusetts Institute of Technology, Cambridge, MA, United States*
- ⁵⁸ *University of Cincinnati, Cincinnati, OH, United States*
- ⁵⁹ *University of Maryland, College Park, MD, United States*
- ⁶⁰ *Syracuse University, Syracuse, NY, United States*
- ⁶¹ *Pontifícia Universidade Católica do Rio de Janeiro (PUC-Rio), Rio de Janeiro, Brazil, associated to ²*
- ⁶² *University of Chinese Academy of Sciences, Beijing, China, associated to ³*
- ⁶³ *Institute of Particle Physics, Central China Normal University, Wuhan, Hubei, China, associated to ³*
- ⁶⁴ *Departamento de Física, Universidad Nacional de Colombia, Bogota, Colombia, associated to ⁸*
- ⁶⁵ *Institut für Physik, Universität Rostock, Rostock, Germany, associated to ¹²*

- ⁶⁶ *National Research Centre Kurchatov Institute, Moscow, Russia, associated to* ³²
- ⁶⁷ *Yandex School of Data Analysis, Moscow, Russia, associated to* ³²
- ⁶⁸ *Instituto de Fisica Corpuscular (IFIC), Universitat de Valencia-CSIC, Valencia, Spain, associated to* ³⁷
- ⁶⁹ *Van Swinderen Institute, University of Groningen, Groningen, The Netherlands, associated to* ⁴²
- ^a *Universidade Federal do Triângulo Mineiro (UFMT), Uberaba-MG, Brazil*
- ^b *Laboratoire Leprince-Ringuet, Palaiseau, France*
- ^c *P.N. Lebedev Physical Institute, Russian Academy of Science (LPI RAS), Moscow, Russia*
- ^d *Università di Bari, Bari, Italy*
- ^e *Università di Bologna, Bologna, Italy*
- ^f *Università di Cagliari, Cagliari, Italy*
- ^g *Università di Ferrara, Ferrara, Italy*
- ^h *Università di Urbino, Urbino, Italy*
- ⁱ *Università di Modena e Reggio Emilia, Modena, Italy*
- ^j *Università di Genova, Genova, Italy*
- ^k *Università di Milano Bicocca, Milano, Italy*
- ^l *Università di Roma Tor Vergata, Roma, Italy*
- ^m *Università di Roma La Sapienza, Roma, Italy*
- ⁿ *Università della Basilicata, Potenza, Italy*
- ^o *AGH - University of Science and Technology, Faculty of Computer Science, Electronics and Telecommunications, Kraków, Poland*
- ^p *LIFAELS, La Salle, Universitat Ramon Llull, Barcelona, Spain*
- ^q *Hanoi University of Science, Hanoi, Viet Nam*
- ^r *Università di Padova, Padova, Italy*
- ^s *Università di Pisa, Pisa, Italy*
- ^t *Scuola Normale Superiore, Pisa, Italy*
- ^u *Università degli Studi di Milano, Milano, Italy*
- [†] *Deceased*